Hindawi
International Journal of Antennas and Propagation
Volume 2017, Article ID 1260973, 11 pages
https://doi.org/10.1155/2017/1260973

Research Article

Wideband RCS Reduction of Microstrip Array Antenna Based on Absorptive Frequency Selective Surface and Microstrip Resonators

Jingjing Xue, Wen Jiang, and Shuxi Gong

National Laboratory of Antennas and Microwave Technology, Xidian University, Xi'an, Shaanxi 710071, China

Correspondence should be addressed to Wen Jiang; jw13@vip.qq.com

Received 21 January 2017; Revised 29 March 2017; Accepted 2 April 2017; Published 2 May 2017

Academic Editor: N. Nasimuddin

An approach for wideband radar cross section (RCS) reduction of a microstrip array antenna is presented and discussed. The scheme is based on the microstrip resonators and absorptive frequency selective surface (AFSS) with a wideband absorptive property over the low band 1.9–7.5 GHz and a transmission characteristic at high frequency 11.05 GHz. The AFSS is designed to realize the out-of-band RCS reduction and preserve the radiation performance simultaneously, and it is placed above the antenna with the operating frequency of 11.05 GHz. Moreover, the microstrip resonators are loaded to obtain the in-band RCS reduction. As a result, a significant RCS reduction from 1.5 GHz to 13 GHz for both types of polarization has been accomplished. Compared with the reference antenna, the simulated results exhibit that the monostatic RCS of the proposed array antenna in x- and y-polarization can be reduced as much as 17.6 dB and 21.5 dB, respectively. And the measured results agree well with the simulated ones.

1. Introduction

With the rapid development of the defense electronics and advanced detection technology, much attention has been paid to the reduction of radar cross section (RCS). For a low-observable platform, antennas are the main contribution to the total RCS [1]. Not all common approaches to reduce RCS are suitable for antennas on account of its feature to radiate and receive electromagnetic wave effectively. Thus it is a challenge to realize a remarkable RCS reduction and preserve the radiation characteristic simultaneously.

Several methods have been proposed in literatures to reduce the RCS of antenna. Shaping the radiation patch or ground plane [2, 3] is one way to obtain the low RCS antennas, while the RCS reduction is usually in a relatively narrow frequency band and the reduction effect is not ideal. With the random or ladder arrangement of antenna array elements [4, 5], the RCS of antenna array can be reduced, which provides an effective method to reduce the RCS of multielement arrays. The reactive impendence surface (RIS) is introduced in [6–8] and a two-layer mushroom-like RIS is presented in [9] to realize the antenna miniaturization and improve the radiation performance. And the mushroom-like structures also can be utilized to reduce RCS of patch antenna arrays [10]. Chessboard configurations of the perfect electric conductor (PEC) and artificial magnetic conductors (AMC) obtain a 180° (±30°) phase difference of the reflected waves in a narrow band, realizing the RCS reduction in the corresponding band. By replacing the PEC and AMC with two different AMC cells, 180° (±30°) reflection phase difference is obtained in a broadband frequency region, achieving the wideband RCS reduction [11]. Another approach based on the principle of passive cancellation is the implementation of the polarization conversion metasurfaces [12–14]. With the proper arrangement of the polarization conversion metasurfaces cells, 180° (±30°) phase difference of the reflected waves can be realized, thus reducing the RCS.

The radar absorbing material (RAM) absorbs the incoming wave and converts the energy into heat, but the antenna radiation performance will be affected. Frequency selective surface (FSS) is widely employed as a band-pass radome to deflect the out-of-band signals away from the threat angular domain [15, 16], or a band-stop ground plane of antennas to reduce out-of-band RCS [17]. However, FSS is only suitable

for out-of-band RCS reduction. In 1995, a concept of absorptive/transmissive radome was presented [18], combining the resistive absorber with a band-pass FSS at the bottom. Instead of reflecting the electromagnetic wave, the out-of-band energy is consumed with the resistors, and the in-band signal is transparent with little loss. Different designs of the absorptive/transmissive radome composed of the resistive layer and band-pass FSS were proposed [19–22]. In [19, 20], the absorptive/transmissive radome has a lower pass-band and a higher wide absorbing band. In [21, 22], the absorptive frequency selective surface (AFSS) with the absorbing band locating lower than the transmission band is introduced, but the designs are polarization dependent because of the asymmetric structure. A planar stealthy radome composed of AFSS is applied to a microstrip antenna to absorb the out-of-band electromagnetic waves, not considering the in-band RCS reduction [23].

In this paper, a low RCS microstrip array antenna based on the AFSS and microstrip resonators is presented. The design of the AFSS is introduced in Section 2. Different from the AFSS in [21, 22], the proposed AFSS has the advantage of polarization stability and wider absorbing band. In order to illustrate the effect of AFSS, reference antenna only with AFSS placed above it is analyzed in Section 3, reducing the out-of-band RCS. Then, reference antenna loaded with AFSS and microstrip resonators is presented in Section 4, realizing a wideband RCS reduction from 1.5 GHz to 13 GHz for x- and y-polarization. The prototypes of reference and proposed antenna are fabricated and measured to verify the reliability and performance of the proposed design. All simulation works are accomplished by using Ansoft's High Frequency Solution Solver (HFSS) software.

2. AFSS Design

Traditional absorber consists of a resistive absorbing layer, substrate layer, and metal reflection plate. By replacing the metal reflection plate with a band-pass FSS, an AFSS can be designed. The proposed AFSS realizes a wide absorptive property over the low band and a good transmission characteristic at high frequency. At high frequency, the same as the resonant frequency of band-pass FSS, the absorber does not work and the signals can transmit. In low frequency band, the absorbing layer resonates and the band-pass FSS acts as the ground plate.

The schematic view of the proposed AFSS unit is shown in Figure 1. It consists of a resistive absorbing layer and a band-pass FSS layer separated by a PMI foam with the permittivity closed to air and thickness of $h = 14$ mm. The resistive layer and FSS layer are printed on the substrates with the permittivity of 2.2 and thickness of 0.254 mm. It is worth mentioning that the proposed AFSS gains some advantages over the AFSS in the existing literatures, such as polarization stability and wider absorbing band. The design of the resistive absorbing layer is introduced as follows.

The square-ring-shaped structure is widely utilized to design the metamaterial absorber [24–27], and the equivalent circuit model for arrays of square loops is introduced in [25, 28]. Based on the structure in [25], the structure of the resistive layer in the submitted paper is proposed. The meandering metal lines are designed to realize the miniaturization. The design guidelines of a wideband absorber are introduced in [26]. Following the steps in [26], the resistive layer dimensions can be determined. The detailed parameters of the proposed AFSS are presented in Table 1. Besides, resistance $R1$ and resistance $R2$ in Figure 1 are optimized for optimum frequency responses, which are 10 Ohms and 43 Ohms, respectively.

Table 1: Parameters of the proposed AFSS.

Parameter	Value (mm)
px	17.2
$L1$	4.7
$L5$	1.7
$W1$	0.4
py	17.2
$L2$	1.6
$L6$	2.2
$W2$	0.2
$h2$	0.254
$L3$	1.5
$L7$	1
s	0.3
$h1$	14
$L4$	0.7
$L8$	0.4
$s1$	0.25

The equivalent circuit model of the proposed resistive absorbing layer with metal reflection plate named absorber is presented in Figure 2. Y_0 and Y_{in} are the intrinsic admittance of air and the input admittance of the absorber, respectively. To verify the validity of the equivalent circuit model, the reflectivity performance of the absorber by the circuit model against HFSS software is compared, illuminated in Figure 3. The circuit model is conducted using the values: $R = 235\,\Omega$, $C = 0.3$ pF, and $L = 7.4$ nH. From Figure 3, the results between the circuit model and HFSS simulations are in good agreement. And there are two resonances within the operating frequency band. Based on the two resonances, the proposed AFSS realizes the wideband absorbing performance.

An important step in the FSS design is the choice of the element form, which affects the operating bandwidth and polarization stability of FSS. Generally, various FSS can be applied in the AFSS design if the FSS satisfies two characteristics: (1) in the transmission band, the insertion loss of the AFSS should be as small as possible for the effective transmission of signal; (2) in the absorbing band, the reflection property of the FSS should be as close as possible to the metal plate. The band-pass FSS element dimensions are determined using FSS design theory [29]. Considering the effect between the absorbing layer and FSS layer, the array and spacing of FSS element are optimized to realize the lower insertion loss.

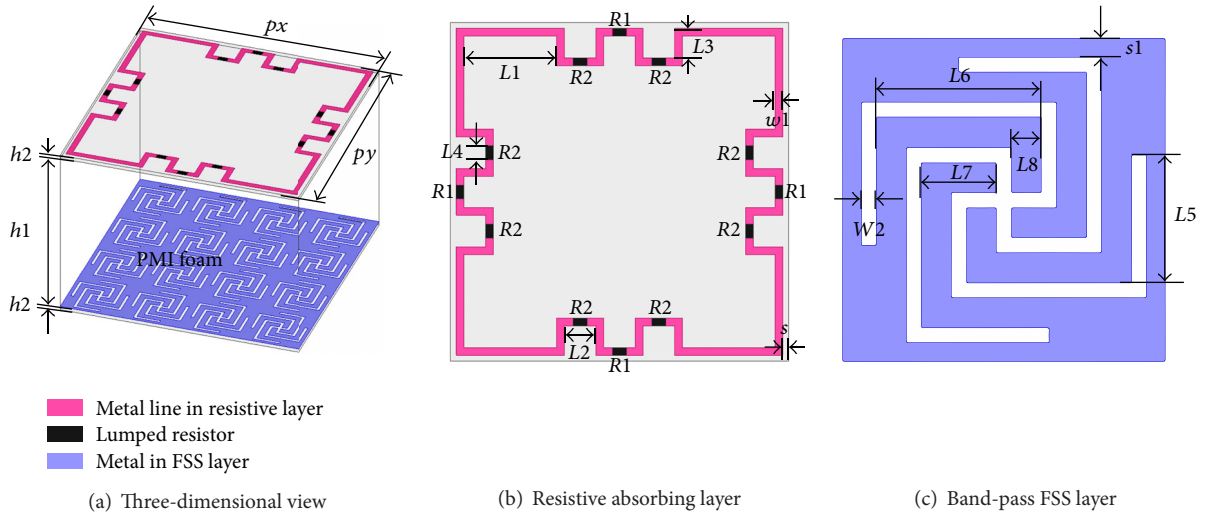

(a) Three-dimensional view (b) Resistive absorbing layer (c) Band-pass FSS layer

FIGURE 1: Schematic view of the proposed AFSS unit.

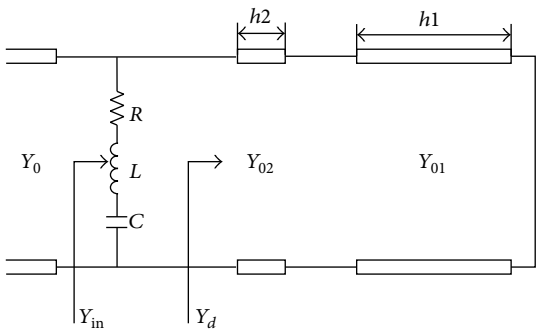

FIGURE 2: Equivalent circuit model of the proposed resistive absorbing layer with metal reflection plate.

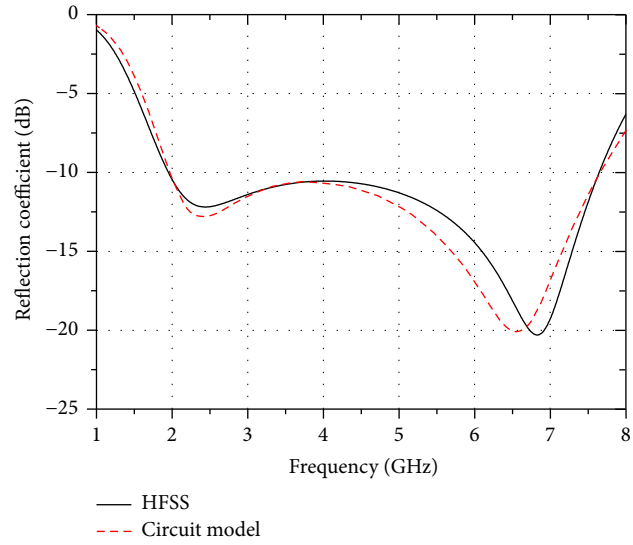

FIGURE 3: Reflection coefficients calculated from the equivalent circuit model and HFSS.

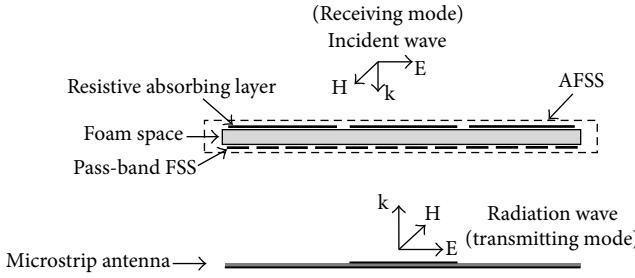

FIGURE 4: Profile sketch representing the receiving and transmitting modes.

The performance of the proposed AFSS is analyzed both in receiving and in transmitting mode. The receiving mode refers to a plane wave irradiating on the absorbing side. The transmitting mode means that the antenna is radiating towards the band-pass FSS side. The receiving and transmitting mode are introduced in Figure 4. When the AFSS works in the receiving mode, a strong current will be induced on the absorbing layer and the energy is consumed with the lumped resisters. Thus the RCS reduction can be realized. In the transmitting mode, the operation frequency of the antenna is the same as the resonant frequency of band-pass FSS, preserving the radiation characteristics of the antenna.

The reflection and transmission coefficients of the AFSS in receiving and in transmitting mode are shown in Figure 5. From Figure 5(a), it can be seen that the −10 dB absorption band is 1.9–7.5 GHz, and the transmission frequency is 11.05 GHz with the insertion loss of 0.8 dB. In Figure 5(b), the reflection coefficients over the low band in transmitting mode are undoubtedly different from the one obtained in receiving mode. The reason is that the FSS acts as the metal plate over the low band and the energy is totally reflected. From Figure 5, both the receiving and transmitting mode show a good transmission characteristic in the frequency 11.05 GHz, allowing the antenna to receive or transmit signal within its working frequency band. Besides, the plots under x- and y-polarization completely overlap, showing an excellent polarization stability.

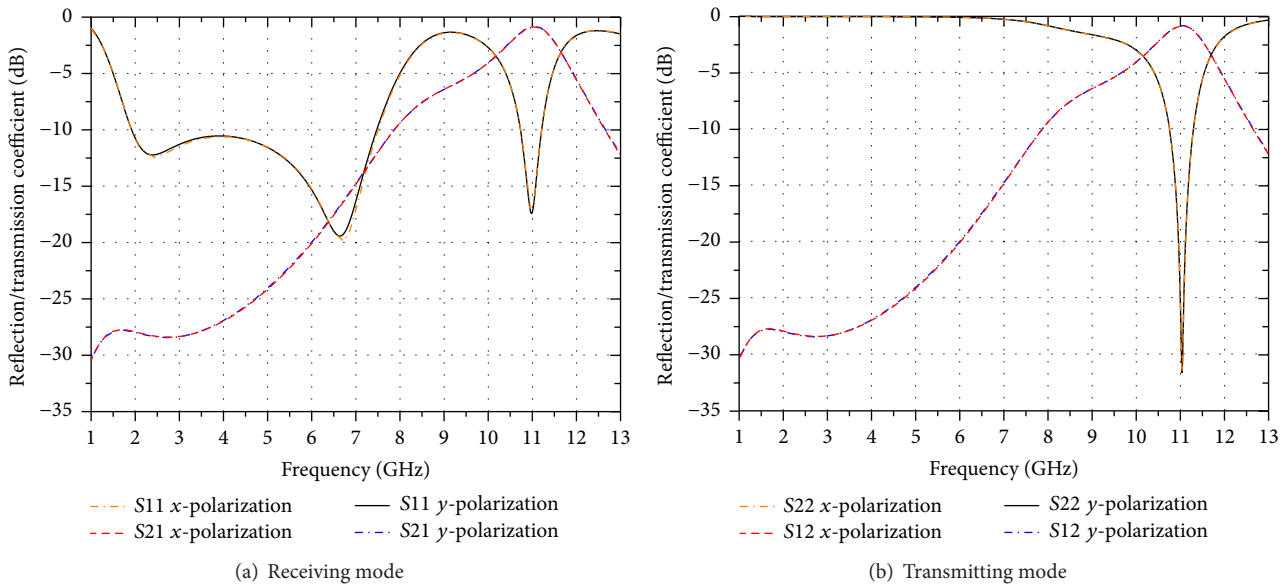

(a) Receiving mode (b) Transmitting mode

Figure 5: Simulated reflection and transmission coefficients of AFSS.

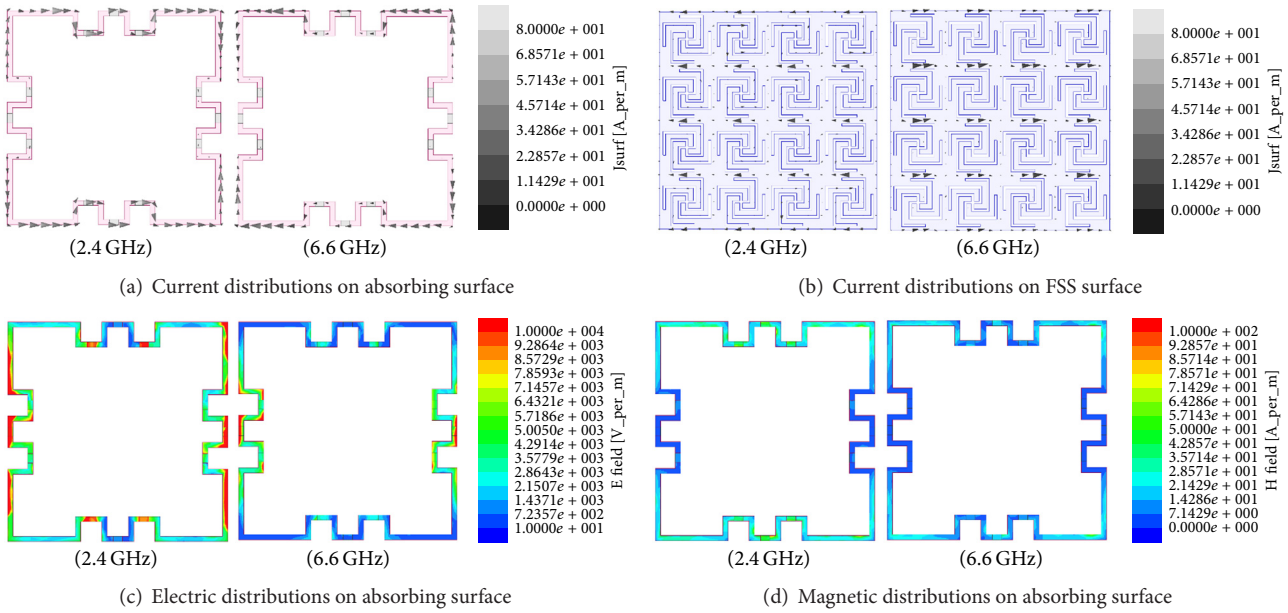

(a) Current distributions on absorbing surface (b) Current distributions on FSS surface

(c) Electric distributions on absorbing surface (d) Magnetic distributions on absorbing surface

Figure 6: Surface current and field distributions at different absorption frequencies.

The surface current and field distributions at two resonant frequencies under normal incidence are illustrated in Figure 6. As shown in Figures 6(a) and 6(b), the current directions on the absorbing surface and the FSS surface are antiparallel. These antiparallel currents on the two layers create the magnetic flux and provide the magnetic resonances. From Figures 6(a), 6(c), and 6(d), the current density distribution is consistent with the magnetic field intensity distribution. That is to say, the places with the higher surface current distribution have the greater magnetic field intensity. However, the electric field intensity distribution and the current density distribution follow the opposite trend. The start and end points of the surface current are located in the places where the electric energy density is the highest. The strong electromagnetic absorption properties result from the combined effect of electric and magnetic excitation [30].

Based on the above results, one can deduce that the proposed AFSS could reduce the out-of-band RCS remarkably and preserve the radiation performance of the microstrip antenna at the same time.

3. Integrated Design of Antenna and AFSS

In order to verify the effect of the proposed AFSS on out-of-band RCS reduction, the AFSS is placed above a microstrip array antenna, which is the reference antenna with

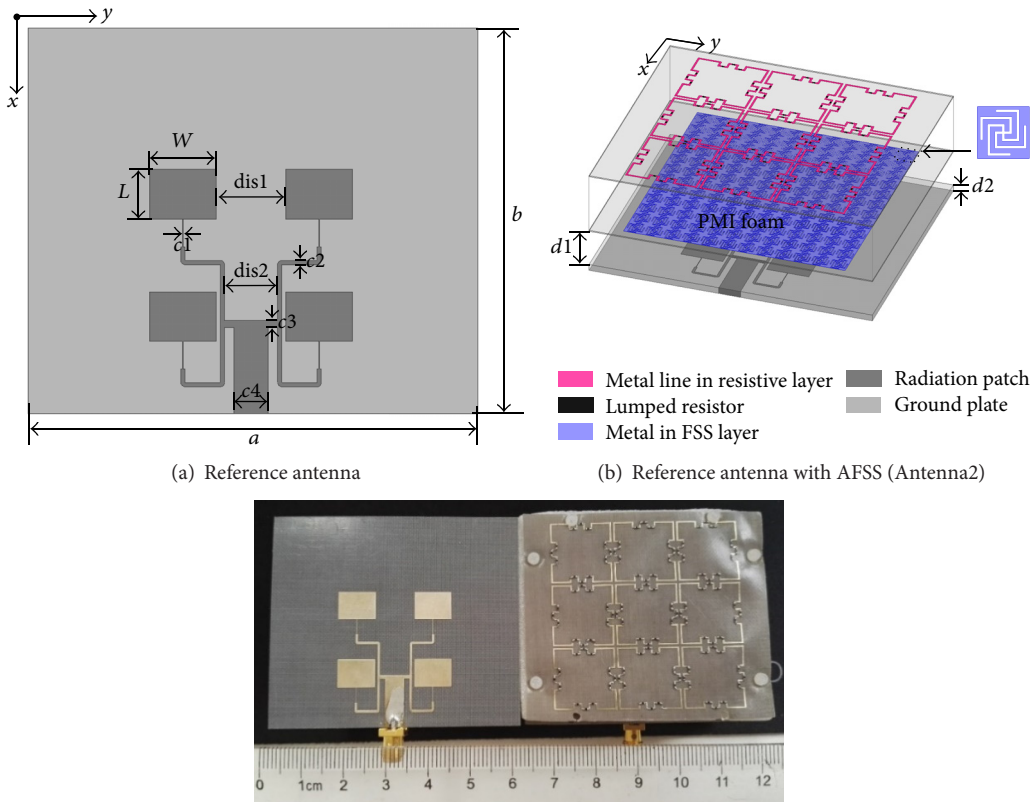

(a) Reference antenna

(b) Reference antenna with AFSS (Antenna2)

(c) Fabricated reference antenna and reference antenna with AFSS (Antenna2)

FIGURE 7: Schematic diagrams of reference antenna and integrated design.

the operation frequency of 11.05 GHz. The schematic diagrams of the reference antenna and the reference antenna with AFSS named Antenna2 are depicted in Figure 7. The reference antenna with the dimension of $a = 66$ mm and $b = 56.6$ mm is four-element microstrip array fed by the microstrip power divider. The microstrip array element and microstrip power divider are printed on the dielectric substrate with the thickness of 1.5 mm and the relative permittivity of 2.65. The AFSS is placed above the reference antenna at a distance of $d1$. Considering the overall dimension of reference antenna, the AFSS is a finite structure with 3×3 resistive absorbing cells and 12×12 band-pass FSS cells on each side. Table 2 exhibits the detailed parameters in Figure 7.

The simulated and measured radiation performances of the reference antenna and Antenna2 are presented in Figure 8. As shown in Figure 8(a), the resonant frequency of Antenna2 is slightly lower than that of the reference antenna and the −10 dB bandwidth is wider than the reference antenna. Specifically, the relative bandwidth ($|S11| \leq -10$ dB) of the reference antenna and Antenna2 is 5.5% and 6.4%, respectively. The measured $|S11|$ has a small shift from the simulated one. This is mainly due to the fabrication tolerance and measurement uncertainty. In Figures 8(b) and 8(c), we can draw a conclusion that the radiation patterns of Antenna2 do not degrade obviously, and the gain loss in the normal direction (z-axis) is 0.8 dB due to the energy consumption with AFSS above the reference antenna. Besides, the measured results agree well with the simulated ones.

TABLE 2: Parameters of reference antenna and integrated design.

Parameter	Value (mm)
a	66
$c1$	0.1
dis1	10.2
b	56.6
$c2$	0.6
dis2	7.8
W	9.8
$c3$	1
$d1$	9
L	7.4
$c4$	5
$d2$	1.5

The simulated and measured monostatic RCS of the two antennas irradiated by x- and y-polarization waves are exhibited to validate the effect of RCS reduction. Figure 9

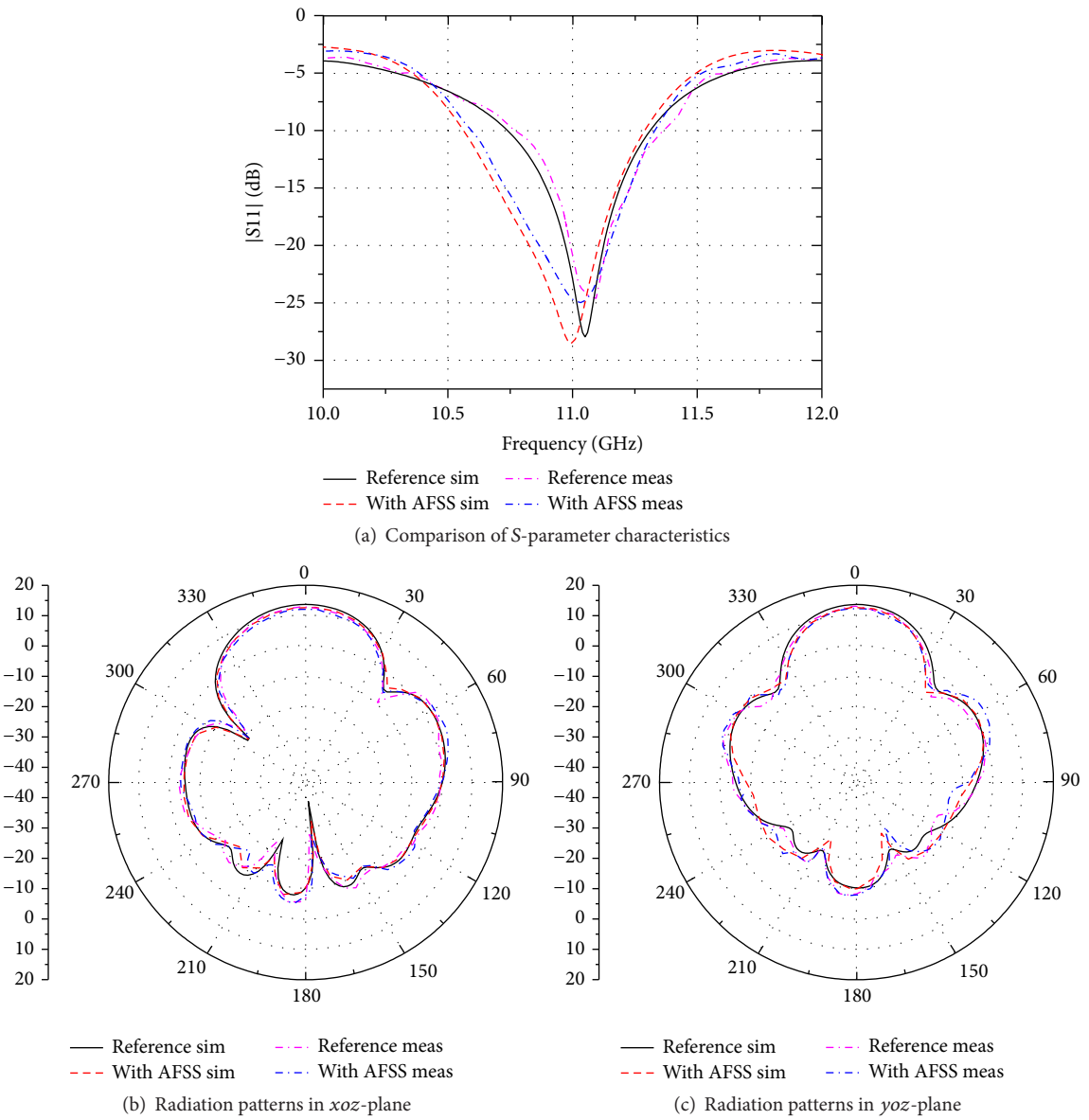

(a) Comparison of *S*-parameter characteristics

(b) Radiation patterns in *xoz*-plane

(c) Radiation patterns in *yoz*-plane

Figure 8: Radiation performance of the reference antenna and the reference antenna with AFSS (Antenna2).

plots the RCS curves versus the frequency for a normal incident plane wave. Figure 9 indicates that a remarkable out-of-band RCS reduction is realized with the help of AFSS, and the monostatic RCS in x- and y-polarization has been reduced as much as 18.0 dB and 24.2 dB, respectively. The measured and simulated monostatic RCS have small differences, while good agreement can be found.

The 3D scattered fields of the two antennas at 4.0 GHz are displayed in Figure 10. Due to the absorbing characteristic of the AFSS, the scattered energy in the region of $z > 0$ is significantly reduced, so that the monostatic RCS in the normal direction can be reduced and the bistatic RCS can be controlled in a certain angle.

The reference antenna with AFSS placed above it can reduce the out-of-band RCS of the reference antenna, while the approach is not effective in reducing the in-band RCS. In order to reduce the in-band RCS, Antenna2 is loaded with microstrip resonators, described in the next section.

4. Integrated Design with Microstrip Resonators

As we all know, microstrip resonators are widely used in the field of microwaves. These microstrip resonators, fed as radiators, are the so-called microstrip antennas. A simple and useful theory using cavity model has been used to analyze the microstrip resonator antennas [31, 32]. According to the cavity model, the resonant frequency of the rectangular resonator can be calculated by

$$f_{mn} = \frac{c}{2\sqrt{\varepsilon_r}} \sqrt{\left(\frac{m}{a}\right)^2 + \left(\frac{n}{b}\right)^2}, \quad (1)$$

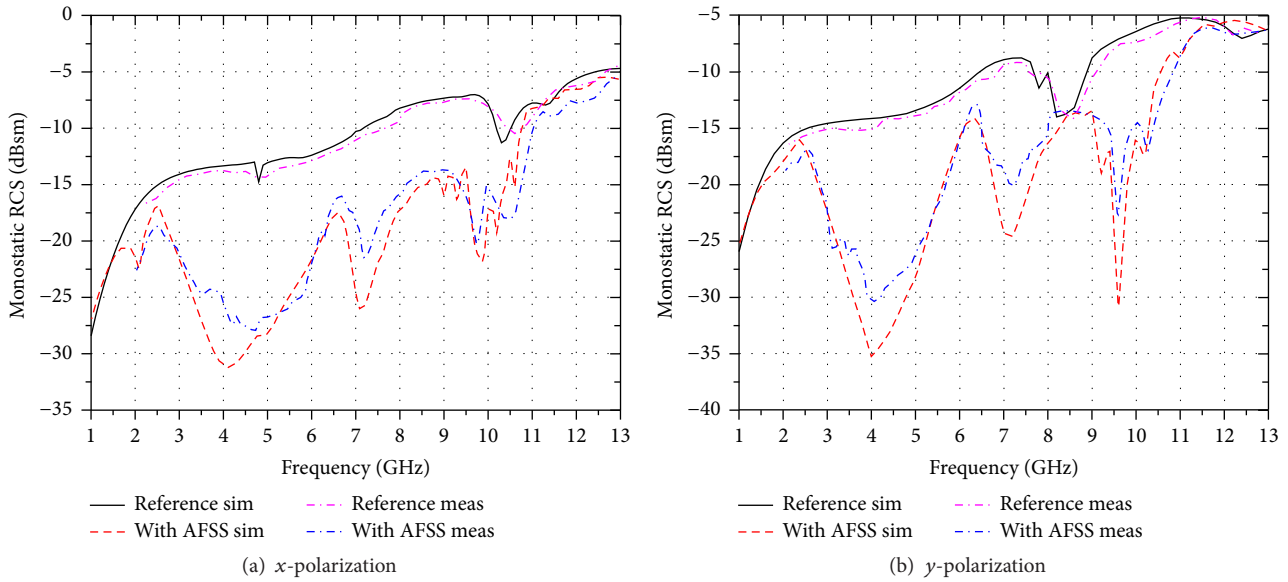

(a) x-polarization (b) y-polarization

Figure 9: Comparison of monostatic RCS between the reference antenna and the reference antenna with AFSS (Antenna2).

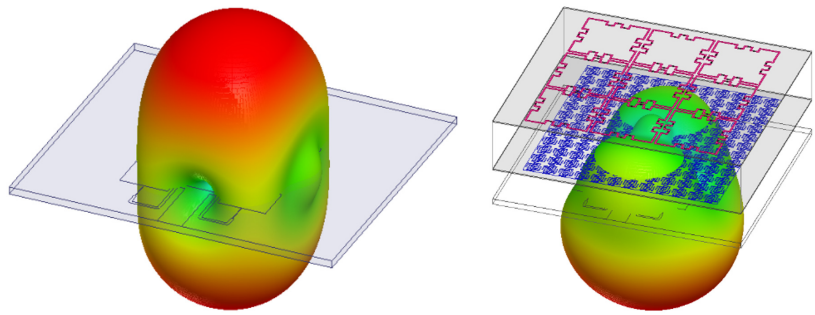

(a) Reference antenna (b) Reference antenna with AFSS (Antenna2)

Figure 10: 3D bistatic scattered fields at 4.0 GHz under normal incidence.

where a and b are the length and width, respectively, ε_r is the relative dielectric constant, and c is the speed of light in vacuum.

The reference antenna with microstrip resonators is shown in Figure 11(a), and the reference antenna with AFSS and microstrip resonators named Antenna3 is exhibited in Figure 11(b). As shown in Figure 11(a), the microstrip resonators and the radiation patch are on the upper side of the dielectric substrate, and the microstrip resonators with the same size are marked with the same number; detailed parameters are shown in Table 3. The resonant frequencies of resonators 1, 2, and 3 are different to obtain a wider RCS reduction.

The current distributions on the surfaces of the resonators and the ground plane for a normally incident y-polarized wave at 11 GHz are shown in Figure 12. It is observed that the current distributions on the microstrip resonators and the ground plane are in the opposite direction, which indicates a 180° reflection phase difference between them. It proves that scattering field of the resonators can cancel the scattering field of the ground plane. The resonators can reduce the in-band RCS based on the principle of passive cancellation.

Table 3: Parameters of reference antenna with microstrip resonators.

Parameter	Value (mm)
$a1$	12
$a3$	6
$b1$	9
$b3$	6
$a2$	8
$a4$	11
$b2$	7
$b4$	9
$d3$	2.8
$d4$	2

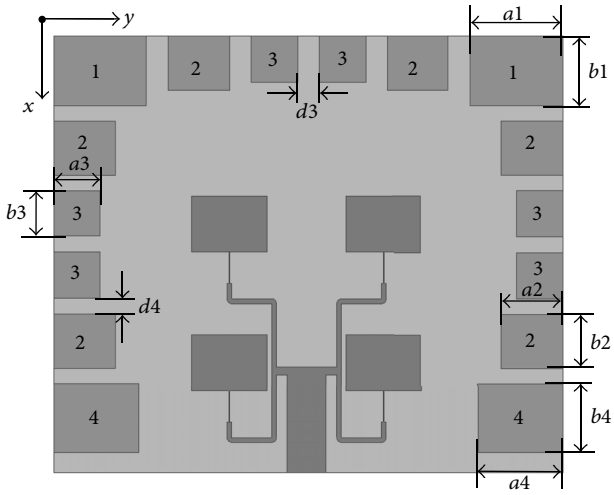

(a) Reference antenna with microstrip resonators

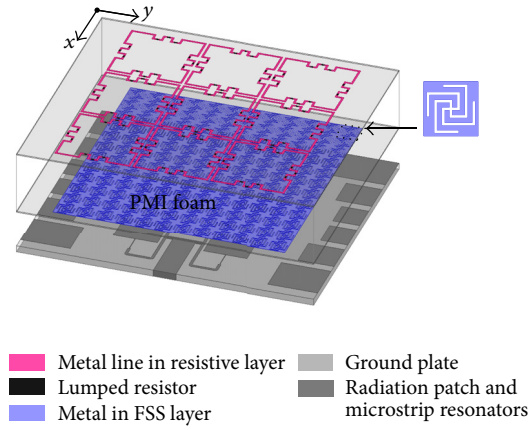

(b) Reference antenna with AFSS and microstrip resonators (Antenna3)

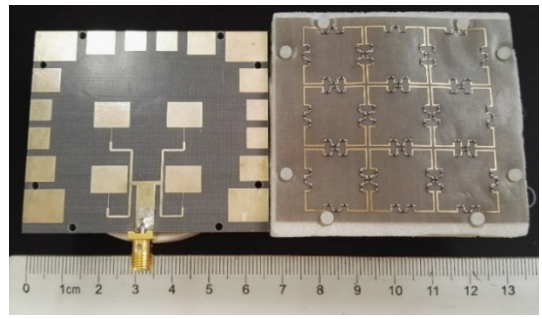

(c) Fabricated reference antenna with AFSS and microstrip resonators (Antenna3)

Figure 11: Schematic diagrams of the proposed design.

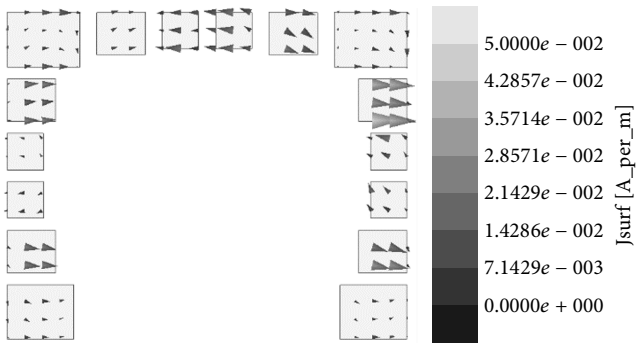

(a) On the surfaces of the resonators

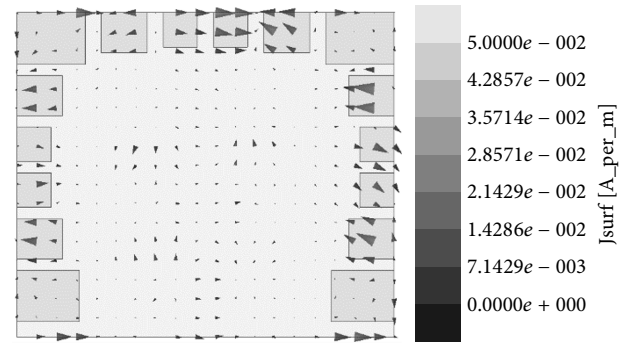

(b) On the surfaces of the ground plane

Figure 12: Current distributions for a normally incident y-polarized wave at 11 GHz.

The simulated and measured radiation properties of the reference antenna and Antenna3 are plotted in Figure 13. Considering the results in Figures 8(a) and 13(a), the slight shift of the resonant frequency and the increase of the −10 dB bandwidth are due to the influence between the antenna and AFSS. Besides, the resonance depth of |S11| is better and the impedance matching is improved, owing to the coupling between the microstrip resonators and the radiation patch. Compared with Figures 8(b) and 8(c), the radiation patterns in Figures 13(b) and 13(c) do not change obviously. Compared with Antenna2, the gain of Antenna3 in the normal direction (z-axis) increases by 0.3 dB because of the improvement of impedance matching; thus the gain loss of Antenna3 is 0.5 dB in contrast to the reference antenna. Similarly,

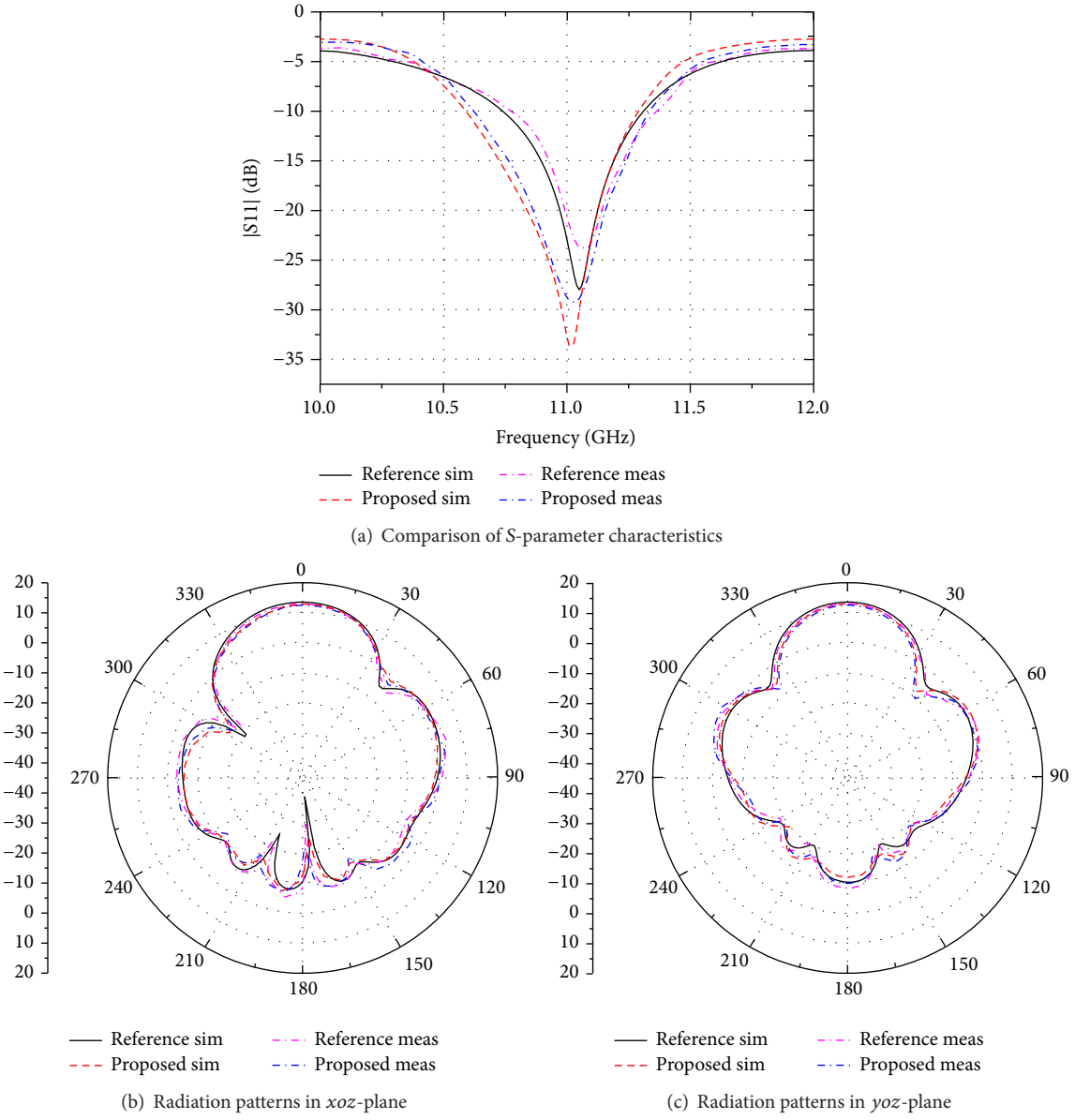

(a) Comparison of S-parameter characteristics

(b) Radiation patterns in xoz-plane

(c) Radiation patterns in yoz-plane

Figure 13: Radiation performance of the reference antenna and the reference antenna with AFSS and microstrip resonators (Antenna3).

the measured results are in good agreement with the simulated ones.

The comparison of monostatic RCS between the reference antenna and Antenna3 is displayed in Figure 14. In Figure 14, a notable RCS reduction from 1.5 GHz to 13 GHz for both types of polarization has been accomplished. Compared with the results in Figure 9, the in-band RCS reduction is improved, and the RCS of Antenna3 in x- and y-polarization can be reduced as much as 17.6 dB and 21.5 dB, respectively. The reasons for the difference between simulated and measured results are fabrication tolerance and the measurement setup.

5. Conclusion

A polarization independent and wideband RCS reduction method of microstrip array antenna is proposed. The AFSS with absorptive property over low band 1.9–7.5 GHz and transmissive performance at 11.05 GHz is utilized to reduce the out-of-band RCS and maintain the radiation performance at the same time. Moreover, the microstrip resonators are employed to obtain the in-band RCS reduction. Consequently, an excellent RCS reduction from 1.5 GHz to 13 GHz for both types of polarization is achieved, and the monostatic RCS of the proposed array antenna in x- and y-polarization can be reduced as much as 17.6 dB and 21.5 dB, respectively. With these outstanding features, the proposed approach is effective and has potential for antenna stealth designs in low RCS platforms.

Conflicts of Interest

The authors declare that they have no conflicts of interest.

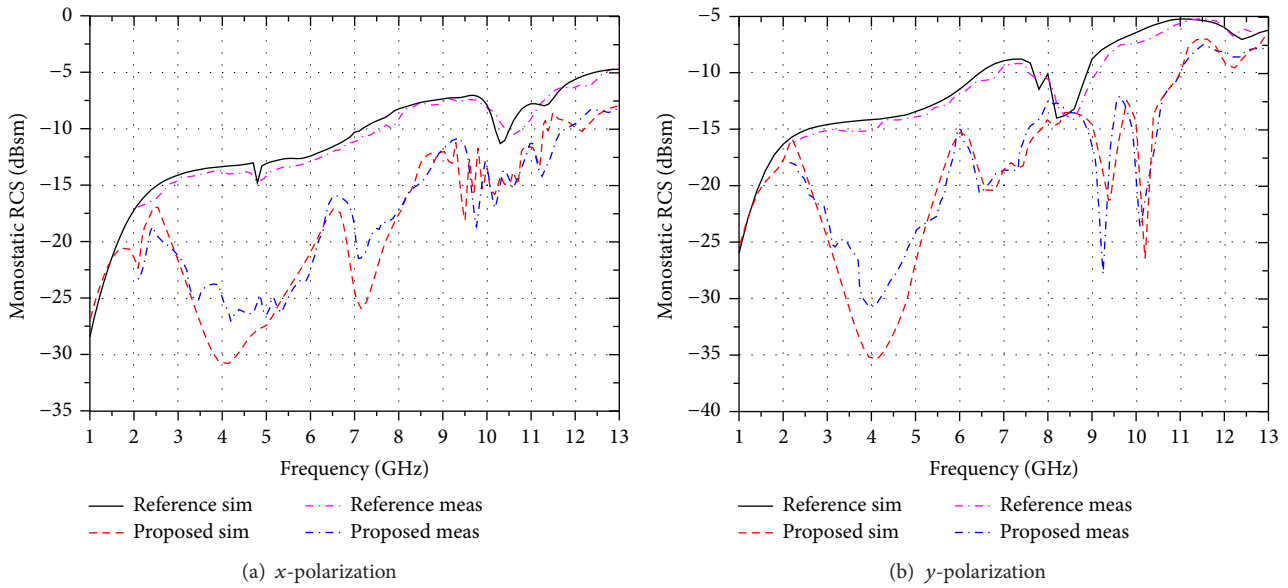

(a) x-polarization (b) y-polarization

FIGURE 14: Comparison of monostatic RCS between the reference antenna and the reference antenna with AFSS and microstrip resonators (Antenna3).

Acknowledgments

This work was supported by National Basic Research Program of China-973 Program 2015CB857100, National Natural Science Foundation of China (nos. 61401327, 61471278), and the Foundation of Chinese Academy of Space Technology (CAST 2015-11).

References

[1] E. F. Knott, J. F. Shaeffer, and M. T. Tuley, *Radar Cross Section*, IET Digital Library, 2004.

[2] X. He, T. Chen, and X. Wang, "A novel low RCS design method for X-band Vivaldi antenna," *International Journal of Antennas and Propagation*, vol. 2012, Article ID 218681, 6 pages, 2012.

[3] W. Jiang, T. Hong, and S. X. Gong, "Research on the scattering characteristics and the RCS reduction of circularly polarized microstrip antenna," *International Journal of Antennas and Propagation*, vol. 2013, Article ID 735847, 9 pages, 2013.

[4] P. Yang, F. Yan, F. Yang, and T. Dong, "Microstrip phased-array in-band RCS reduction with a random element rotation technique," *IEEE Transactions on Antennas and Propagation*, vol. 64, no. 6, pp. 2513–2518, 2016.

[5] X. He, S. Huang, T. Chen, and Y. Yang, "Ladder arrangement method for stealth design of Vivaldi antenna array," *International Journal of Antennas and Propagation*, vol. 2013, Article ID 295767, 7 pages, 2013.

[6] H. Mosallaei and K. Sarabandi, "Antenna miniaturization and bandwidth enhancement using a reactive impedance substrate," *IEEE Transactions on Antennas and Propagation*, vol. 52, no. 9, pp. 2403–2414, 2004.

[7] Y. Dong, H. Toyao, and T. Itoh, "Compact circularly-polarized patch antenna loaded with metamaterial structures," *IEEE Transactions on Antennas and Propagation*, vol. 59, no. 11, pp. 4329–4333, 2011.

[8] K. Agarwal, Nasimuddin, and A. Alphones, "RIS-based compact circularly polarized microstrip antennas," *IEEE Transactions on Antennas and Propagation*, vol. 61, no. 2, pp. 547–554, 2013.

[9] J. Wu and K. Sarabandi, "Reactive impedance surface TM mode slow wave for patch antenna miniaturization [AMTA corner]," *IEEE Antennas and Propagation Magazine*, vol. 56, no. 6, pp. 279–293, 2014.

[10] P. K. Panda and D. Ghosh, "Mushroom-like EBG structures for reducing RCS of patch antenna arrays," in *Proceedings of the International Conference on Microwave and Photonics (ICMAP '13)*, pp. 1–4, IEEE, Dhanbad, India, December 2013.

[11] Y. Zheng, J. Gao, X. Cao, Z. Yuan, and H. Yang, "Wideband RCS reduction of a microstrip antenna using artificial magnetic conductor structures," *IEEE Antennas and Wireless Propagation Letters*, vol. 14, pp. 1582–1585, 2015.

[12] Y. Jia, Y. Liu, Y. J. Guo, K. Li, and S. Gong, "Broadband polarization rotation reflective surfaces and their applications to RCS reduction," *IEEE Transactions on Antennas and Propagation*, vol. 64, no. 1, pp. 179–188, 2016.

[13] Y. Liu, K. Li, Y. Jia, Y. Hao, S. Gong, and Y. J. Guo, "Wideband RCS reduction of a slot array antenna using polarization conversion metasurfaces," *IEEE Transactions on Antennas and Propagation*, vol. 64, no. 1, pp. 326–331, 2016.

[14] Y. Liu, Y. Hao, K. Li, and S. Gong, "Radar cross section reduction of a microstrip antenna based on polarization conversion metamaterial," *IEEE Antennas and Wireless Propagation Letters*, vol. 15, pp. 80–83, 2016.

[15] H. Zhou, S. Qu, B. Lin et al., "Filter-antenna consisting of conical FSS radome and monopole antenna," *IEEE Transactions on Antennas and Propagation*, vol. 60, no. 6, pp. 3040–3045, 2012.

[16] B.-Q. Lin, F. Li, Q.-R. Zheng, and Y.-S. Zen, "Design and simulation of a miniature thick-screen frequency selective surface radome," *IEEE Antennas and Wireless Propagation Letters*, vol. 8, pp. 1065–1068, 2009.

[17] M. Zahir Joozdani, M. Khalaj Amirhosseini, and A. Abdolali, "Wideband radar cross-section reduction of patch array

antenna with miniaturised hexagonal loop frequency selective surface," *Electronics Letters*, vol. 52, no. 9, pp. 767–768, 2016.

[18] W. S. Arceneaux, R. D. Akins, and W. B. May, "Absorptive/transmissive radome," US Patent 5,400,043, 1995.

[19] Q. Chen, J. Bai, L. Chen, and Y. Fu, "A miniaturized absorptive frequency selective surface," *IEEE Antennas and Wireless Propagation Letters*, vol. 14, pp. 80–83, 2015.

[20] B. Yi, P. Liu, G. Li, and Y. Dong, "Design of miniaturized and ultrathin absorptive/transmissive radome with wideband absorbing property," *Microwave and Optical Technology Letters*, vol. 58, no. 8, pp. 1870–1875, 2016.

[21] Q. Chen, L. Chen, J. Bai, and Y. Fu, "Design of absorptive frequency selective surface with good transmission at high frequency," *Electronics Letters*, vol. 51, no. 12, pp. 885–886, 2015.

[22] Q. Chen, L. Liu, L. Chen, J. Bai, and Y. Fu, "Absorptive frequency selective surface using parallel LC resonance," *Electronics Letters*, vol. 52, no. 6, pp. 418–419, 2016.

[23] Q. Chen and Y. Fu, "A planar stealthy antenna radome using absorptive frequency selective surface," *Microwave and Optical Technology Letters*, vol. 56, no. 8, pp. 1788–1792, 2014.

[24] C. Huang, W. Pan, X. Ma, and X. Luo, "Wideband radar cross-section reduction of a stacked patch array antenna using metasurface," *IEEE Antennas and Wireless Propagation Letters*, vol. 14, pp. 1369–1372, 2015.

[25] S. Ghosh, S. Bhattacharyya, and K. V. Srivastava, "Design and analysis of a broadband single layer circuit analog absorber," in *Proceedings of the 46th European Microwave Conference (EuMC '16)*, pp. 584–587, London, UK, October 2016.

[26] Y. Shang, Z. Shen, and S. Xiao, "On the design of single-layer circuit analog absorber using double-square-loop array," *IEEE Transactions on Antennas and Propagation*, vol. 61, no. 12, pp. 6022–6029, 2013.

[27] J. Yang and Z. Shen, "A thin and broadband absorber using double-square loops," *IEEE Antennas and Wireless Propagation Letters*, vol. 6, pp. 388–391, 2007.

[28] R. J. Langley and E. A. Parker, "Equivalent circuit model for arrays of square loops," *Electronics Letters*, vol. 18, no. 7, pp. 294–296, 1982.

[29] B. A. Munk, *Frequency Selective Surfaces: Theory and Design*, John Wiley & Sons, New York, NY, USA, 2000.

[30] X. Shen, T. J. Cui, J. Zhao, H. F. Ma, W. X. Jiang, and H. Li, "Polarization-independent wide-angle triple-band metamaterial absorber," *Optics Express*, vol. 19, no. 10, pp. 9401–9407, 2011.

[31] A. G. Derneryd and A. G. Lind, "Extended analysis of rectangular microstrip resonator antennas," *IEEE Transactions on Antennas and Propagation*, vol. 27, no. 6, pp. 846–849, 1979.

[32] I. Wolff and N. Knoppik, "Rectangular and circular microstrip disk capacitors and resonators," *IEEE Transactions on Microwave Theory and Techniques*, vol. 22, no. 10, pp. 857–864, 1974.